

Spin dynamics of $\text{La}_{0.7}\text{Ba}_{0.3}\text{MnO}_3$ Tapan Chatterji,^{1,2} L. P. Regnault,³ and W. Schmidt⁴¹*Institut Laue-Langevin, BP 156, 38042 Grenoble Cedex 9, France*²*Max-Planck-Institut für Physik Komplexer Systeme, Dresden, Germany*³*Centre d'Etudes Nucleaires, DRFMC/SPSMS-MDN, 38054 Grenoble Cedex 9, France*⁴*Institut für Festkörperforschung, Forschungszentrum Jülich, Jülich, Germany*

(Received 25 April 2002; published 12 December 2002)

We have done inelastic neutron scattering investigations of the magnetic excitations in the ferromagnetic $\text{La}_{0.7}\text{Ba}_{0.3}\text{MnO}_3$ which shows colossal magnetoresistance (CMR) behavior close to $T_C \approx 350$ K. We have measured the dispersions of the spin waves along [100] and [110] and also their temperature dependence. We have fitted the dispersions with an effective localized spin model to get the nearest-neighbor exchange interaction. We have shown that the effective localized spin model is no longer valid for larger momentum transfer close to the zone boundary at which the spin-waves show softening. Also the spin-wave energy widths are found to be much larger than the instrumental resolution. We argue that the spin-wave softening and damping are generic to the double-exchange ferromagnet including those with large T_C .

DOI: 10.1103/PhysRevB.66.214408

PACS number(s): 75.30.Ds, 75.25.+z, 72.15.Gd

The manganites $\text{Ln}_{1-x}\text{A}_x\text{MnO}_3$ (Ln = Lanthanide atom, A = divalent atom Sr, Ca, Ba, etc.) with the perovskitelike structure have been the subject of intense investigations due to their colossal magnetoresistive (CMR) behavior.^{1,2} LaMnO_3 is an antiferromagnetic insulator. Because of the staggered arrangements of the $d_{x^2-3y^2}$ and $d_{y^2-3x^2}$ orbitals in the a - b plane of the orthorhombic $Pbnm$ structure, the Mn moments are ferromagnetically coupled in this plane. The ferromagnetic a - b planes are antiferromagnetically stacked along the c axis. The evolution of the static and dynamic spin correlations with doping have been well investigated³ in $\text{La}_{1-x}\text{Ca}_x\text{MnO}_3$ and $\text{La}_{1-x}\text{Sr}_x\text{MnO}_3$. These systems at low temperature evolve as a function of doping x from an insulating antiferromagnetic state towards a ferromagnetic insulating (FI) state which in turn transforms into a ferromagnetic metallic (FM) state. For $x < 0.125$ magnetic diffuse scattering indicates charge segregation, with interacting ferromagnetic hole-rich platelets imbedded in a hole-poor matrix. For higher hole doping level $x > 0.125$ the ground state is the ferromagnetic metallic state which shows optimal colossal magnetoresistance (CMR) properties for $x = \frac{1}{3}$.

The standard model, describing the ferromagnetic metallic state of the manganites, is based on the double exchange mechanism⁴⁻⁶ due to the Hund's rule coupling of electrons in the $3d$ shell. It may be described⁷ by a ferromagnetic (FM) Kondo lattice Hamiltonian of the type

$$H = -t \sum_{\langle ij \rangle \sigma} (c_{i\sigma}^\dagger c_{j\sigma} + \text{H.c.}) - \frac{J_H}{S} \sum_i \vec{S}_i \cdot \vec{\sigma}_i \quad (1)$$

under the assumption that in the metallic phase the orbital degrees of freedom are averaged out and enter only through renormalized effective parameters (hopping integral t and Hund's rule coupling strength J_H) of the model. Here $c_{i\sigma}$ describes the itinerant e_g -type electrons with spin $\vec{\sigma}$ and \vec{S} ($S = \frac{3}{2}$) is the spin of the localized t_{2g} -type electrons. Furukawa⁷ calculated the spin wave (SW) excitations of this model in the FM phase within first order of a $1/S$ expansion which corresponds to a Stoner type theory where a constant

exchange field (J_H/S) $\langle \vec{S} \rangle$ leads to an exchange splitting for the e_g conduction electrons. He has also shown that in the limit $J_H/t \gg 1$ the magnon dispersion is equivalent to that of a localized nearest-neighbor Heisenberg model. However, Shannon and Chubukov⁸ have discussed to what extent the double-exchange ferromagnet is equivalent to the Heisenberg ferromagnet. They have argued that this equivalence holds only at infinite S , when spin waves are noninteracting quasiparticles. The interaction between spin waves in the double-exchange ferromagnet is qualitatively different from that in a Heisenberg ferromagnet, for which the spin waves are exact eigenstates of the Hamiltonian. This is due to the fact that the dynamics of the bosonic spin wave modes in the double-exchange ferromagnet is governed by those of the itinerant electrons. The spin excitations in the double-exchange ferromagnet are not true eigenstates of the Hamiltonian and have a finite lifetime even at $T=0$. The existence of a finite density of charge carriers generates a dispersion of the spin waves about the ground state of the double-exchange ferromagnet. The fluctuations of the charge density generate a retarded interaction between these spin waves that is proportional to the charge susceptibility of the itinerant electrons. The magnitude of this interaction as well as its dependence on momentum and frequency are very different from that in the Heisenberg model. Golosov⁹ also constructed $1/S$ spin wave expansion for double exchange ferromagnets at $T=0$ on the assumption of a large Hund's rule coupling J_H and have calculated the corrections to the magnon dispersion law and have also found spin wave damping. The quantum corrections of the double-exchange ferromagnets are in consistency with the earlier numerical results.^{10,11} Recently Motome and Furukawa¹² have identified randomness created by the substitution of the divalent ion (Ca, Sr, Ba, etc.) for a trivalent lanthanide ion (La, Pr, Nd, etc.) as the possible origin of the spin wave damping close to the zone boundary of the double exchange ferromagnetic manganites.

The earlier spin wave investigations¹³ on the double-exchange ferromagnetic manganites $\text{La}_{0.7}\text{Pb}_{0.3}\text{MnO}_3$ led to

the conclusion that a simple nearest-neighbor Heisenberg model accounts for the entire spin-wave dispersion. The authors¹³ found that the spin-waves are well defined in the entire Brillouin zone at 10 K. It is curious that they did not observe spin wave damping at low temperature, although they observed the unusual broadening of the high-frequency spin-waves as the temperature of the sample was raised. This investigation was performed at a spallation neutron source on a time-of-flight neutron spectrometer. One should not speak of a single energy transfer in such measurements but mention the range of energy transfer which is of the order of 8 meV in the typical scan shown by the authors. The lowest “energy transfer” shown in the dispersion curve was about 8 meV. The later investigations on other double-exchange ferromagnets $\text{La}_{0.7}\text{Ca}_{0.3}\text{MnO}_3$, $\text{Pr}_{0.63}\text{Sr}_{0.37}\text{MnO}_3$, and $\text{Nd}_{0.7}\text{Sr}_{0.3}\text{MnO}_3$ showed the presence of softening at the zone-boundary and also damping of the spin waves.^{14,15} However, the authors of Refs. 14,15 argue, by noting the absence of zone-boundary softening and damping for a high- T_C double-exchange ferromagnet $\text{La}_{0.7}\text{Pb}_{0.3}\text{MnO}_3$,¹³ that these features are generic only to low- T_C ferromagnetic manganites. Here we report the spin wave investigations on $\text{La}_{0.7}\text{Ba}_{0.3}\text{MnO}_3$ with a ferromagnetic transition temperature as high as $T_C \approx 350$ K. We have observed both softening and damping of the spin waves in “high- T_C ” $\text{La}_{0.7}\text{Ba}_{0.3}\text{MnO}_3$ even at $T=1.5$ K. We argue from our experimental results that the zone-boundary softening and damping are generic features of the double-exchange ferromagnets including those with high value of T_C .

Although the magnetoresistance measurements on thin films of $\text{La}_{0.67}\text{Ba}_{0.33}\text{MnO}_3$ by von Helmolt *et al.*¹⁶ initiated the interest in this class of materials, bulk samples or single crystals of $\text{La}_{1-x}\text{Ba}_x\text{MnO}_3$ have been much less studied compared to the $\text{La}_{1-x}\text{Ca}_x\text{MnO}_3$ and $\text{La}_{1-x}\text{Sr}_x\text{MnO}_3$ systems. This is probably due to the difficulty in substituting the relatively large Ba ion (1.75 Å) for La (1.50 Å) in LaMnO_3 . The phase diagram of $\text{La}_{1-x}\text{Ba}_x\text{MnO}_3$ has been studied by synthesizing polycrystalline samples¹⁷⁻¹⁹ and investigating them by resistivity, magnetization and x-ray and neutron powder diffraction. No inelastic neutron-scattering investigation has been reported on $\text{La}_{0.7}\text{Ba}_{0.3}\text{MnO}_3$ so far. However, Hall effect and inelastic neutron scattering investigations have been reported²⁰ on a $\text{La}_{0.8}\text{Ba}_{0.2}\text{MnO}_3$ single crystal ($T_C \approx 248$ K) grown by the floating zone method. Neutron scattering investigation is only a minor part of this paper²⁰ which reports only a single constant- Q scan at $T=240$ K. From the absence of the quasielastic central peak in this scan the authors conclude that the concentration of the localized states in $\text{La}_{0.8}\text{Ba}_{0.2}\text{MnO}_3$ is markedly less than in $\text{La}_{1-x}\text{Ca}_x\text{MnO}_3$ or $\text{La}_{1-x}\text{Sr}_x\text{MnO}_3$ and hence charge carriers in extended states dominate the transport properties, at least near T_C . No detailed spin wave dispersion has been reported in this paper.

A $\text{La}_{0.7}\text{Ba}_{0.3}\text{MnO}_3$ single crystal of size $5 \times 5 \times 2$ mm³ was used for the present study. The crystal was grown by the flux method by S. A. Guretskii, A. M. Luginets and N. A. Kalandaand of the Institute of Solid State and Semiconductor Physics, National Academy of Sciences of Belarus, Minsk. The crystal has well-defined reflecting crystallographic

growth faces and is of superior quality compared to the crystals finally obtained by the floating zone method. Resistivity and magnetization measurements showed that the crystal has a ferromagnetic Curie temperature $T_C \approx 350$ K. X-ray measurements showed that $\text{La}_{0.7}\text{Ba}_{0.3}\text{MnO}_3$ at room temperature has a rhombohedrally distorted perovskitelike crystal structure (space group $R\bar{3}c$) with lattice parameters $a=3.901$ Å and $\alpha=89.75^\circ$. In order to check the quality and mosaic spread we mounted the single crystal on the four-circle triple-axis single crystal diffractometer D10 of the Institute Laue-Langevin, Grenoble. The crystal was found to be of excellent quality and had resolution-limited mosaic spread. We measured the temperature variation of a few reflections which showed that the crystal has a ferromagnetic transition temperature $T_C \approx 350$ K and also that at $T_c \approx 180$ K, $\text{La}_{0.7}\text{Ba}_{0.3}\text{MnO}_3$ undergoes a structural phase transition to an orthorhombic phase (space group $Imma$). However, in what follows we have treated $\text{La}_{0.7}\text{Ba}_{0.3}\text{MnO}_3$ as pseudocubic with cubic lattice constant $a=3.90$ Å. Resistivity and magnetization measurements showed that the crystal has a ferromagnetic Curie temperature $T_C \approx 350$ K. Inelastic neutron-scattering experiments were performed on the thermal triple-axis “CRG” spectrometer IN22 and the cold triple-axis “CRG” spectrometer IN12 of the Institut Laue-Langevin. In all these experiments the crystal was either placed inside a conventional helium cryostat or a cryofurnace with its [001] crystallographic axis vertical so that the scattering plane was ($hk0$). On IN22 we used a vertically curved monochromator and a horizontally curved analyzer PG graphite (002) crystals. The horizontal and vertical collimations were $15'-30'-60'-80'$ and $15'-120'-120'-120'$, respectively. The final momentum transfer was kept fixed to the values $k_f = 2.662$ and 4.1 Å⁻¹ for low and high energy transfers, respectively on the experiments with the thermal triple-axis spectrometer IN22. On IN12 we used the following configuration: guide—vertically curved PG(002) monochromator—60'—sample—Be filter—horizontally curved PG(002) analyzer crystal—open detector. The final momentum transfer was kept fixed to $k_f = 1.2$ or 1.3 Å⁻¹.

Figure 1 shows a few typical constant-energy scans from $\text{La}_{0.7}\text{Ba}_{0.3}\text{MnO}_3$ in the ferromagnetic ordered state at low temperature. Figure 2 shows the dispersion of the spin waves in $\text{La}_{0.7}\text{Ba}_{0.3}\text{MnO}_3$ at 1.5 K along [100] obtained from the constant energy and also constant- Q scans. The data of the lower energy and momentum transfer were measured on IN12 whereas those of the higher energy and momentum transfers were measured on IN22. The total spin wave energy band width along [100] is about 35 meV. The dispersion along [100] could not be fitted entirely by a simple Heisenberg model. If one fits the small- q part by

$$\hbar\omega \approx \Delta + Dq^2, \quad (2)$$

one gets $\Delta = 0.20 \pm 0.04$ meV and $D = 393 \pm 7$ meV (*r.l.u.*)² or 152 ± 3 meV Å². The exchange interaction J can be calculated from the relation

$$D = 8\pi^2 JS \quad (3)$$

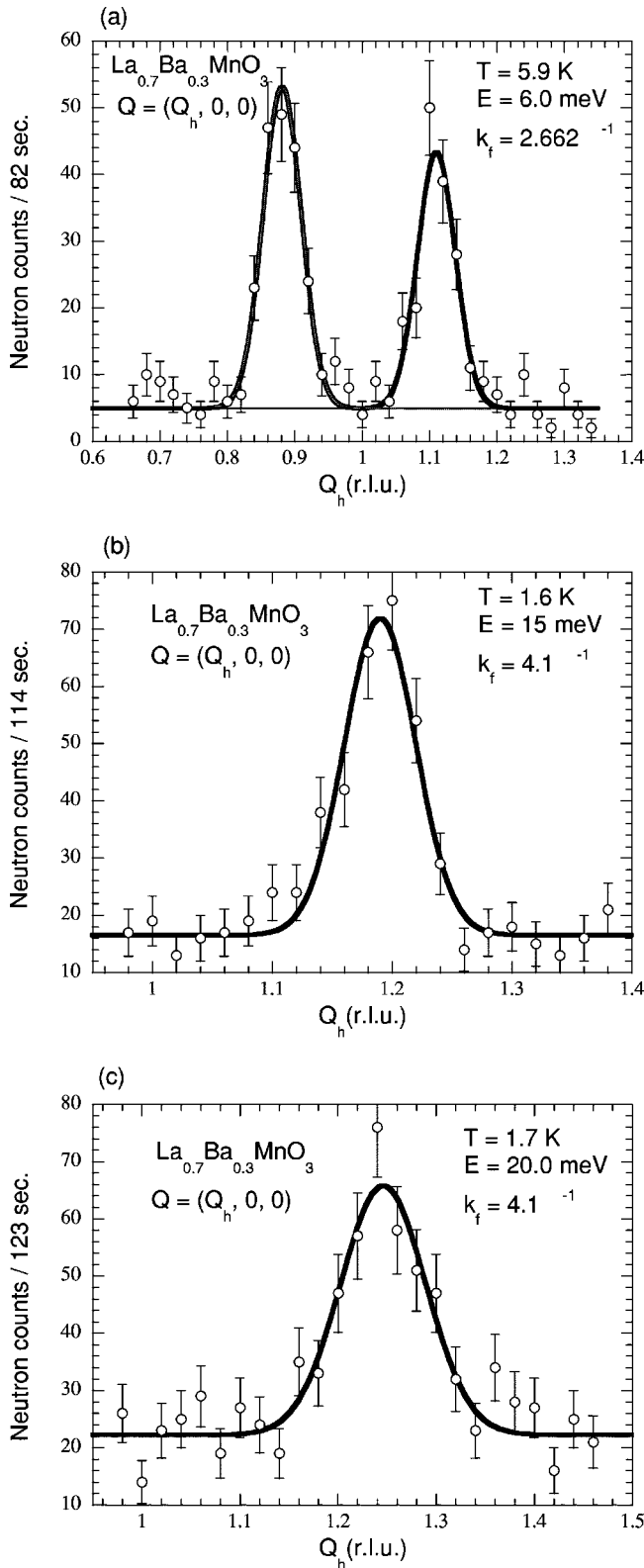


FIG. 1. Typical constant-energy scans from $\text{La}_{0.7}\text{Ba}_{0.3}\text{MnO}_3$ in the ferromagnetic ordered state at low temperature at energy transfers (a) 6.0, (b) 15.0, and (c) 20.0 meV. The final momentum transfer in (a) was 2.662 \AA^{-1} whereas that for (b) and (c) was 4.1 \AA^{-1} .

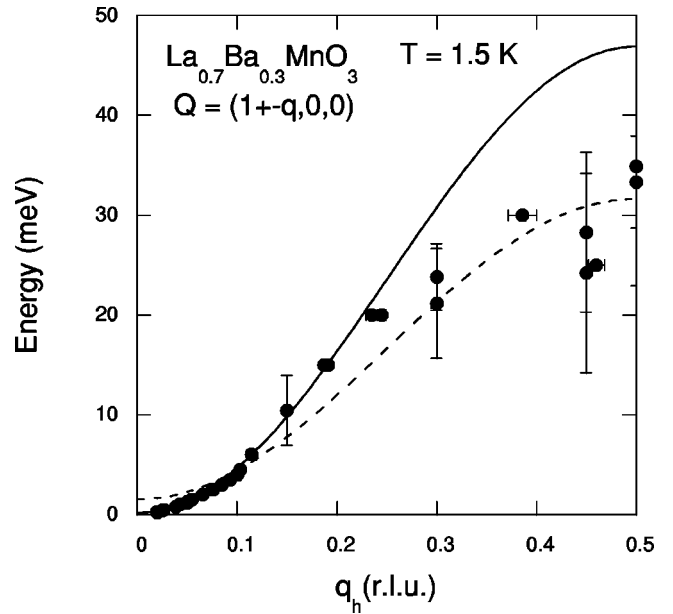


FIG. 2. Dispersion of the acoustic branch of the magnetic excitations in $\text{La}_{0.7}\text{Ba}_{0.3}\text{MnO}_3$ propagating along $[100]$ at $T=1.5 \text{ K}$. The continuous curve has been obtained by determining the gap and the stiffness constant from the low- q data and then using the gap and nearest neighbor exchange constant determined from the spin-wave stiffness constant to calculate the dispersion by Eq. (4). The discrepancy of the calculated and observed dispersion at the zone boundary gives the softening of the spin waves. The vertical lines on some of the data points are the half widths of the energy scans and not the error bars. The dotted curve shows the fit of all data points with Eq. (4) in which both the energy gap Δ and spin-wave bandwidth $4JS$ have been refined. The resulting fit is very bad and gives a wrong value of the gap $\Delta=1.5 \text{ meV}$.

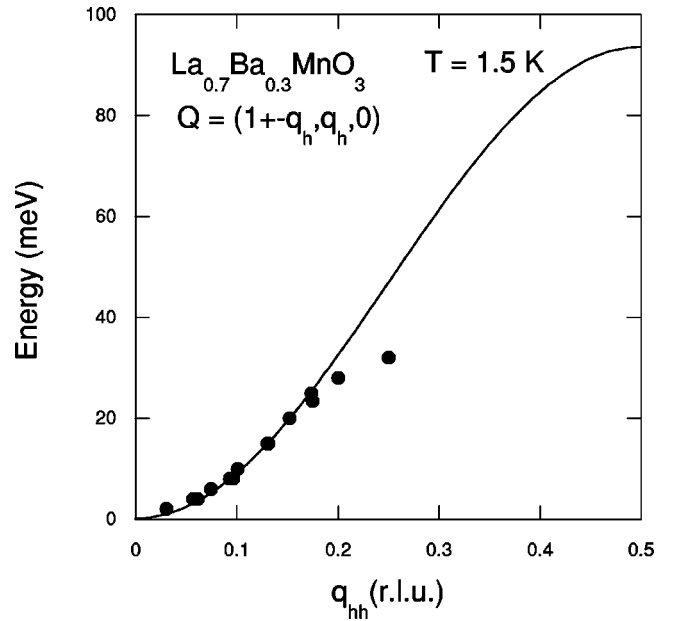


FIG. 3. Dispersion of the acoustic branch of the magnetic excitations in $\text{La}_{0.7}\text{Ba}_{0.3}\text{MnO}_3$ along $[110]$ at $T=1.5 \text{ K}$. The continuous curve shows the calculated dispersion from Eq. (4) by using spin-wave gap $\Delta=0.20 \text{ meV}$ and the nearest-neighbor exchange interaction $JS=5.8 \text{ meV}$ determined along $[100]$ from the low- q data.

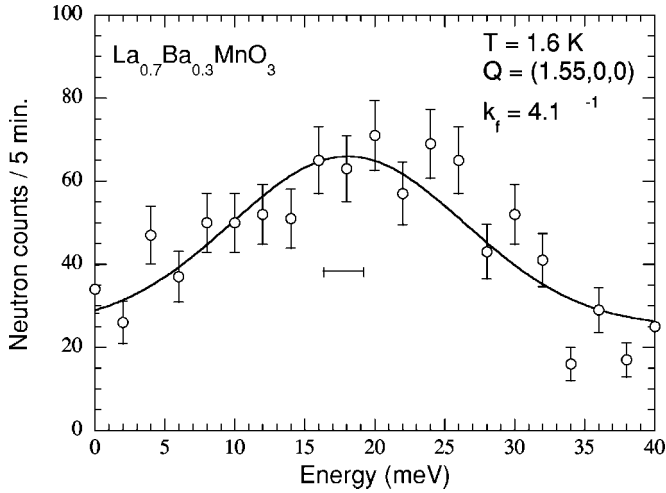


FIG. 4. Typical constant- Q scan of the magnetic excitations in $\text{La}_{0.7}\text{Ba}_{0.3}\text{MnO}_3$ at $T=1.5$ K at $Q=(1.55,0,0)$ close to the zone boundary. The continuous curve is the Gaussian fit of the data. The full-width at the half-maximum (FWHM) of the fitted curve is 20 ± 2 meV which is much larger than the instrumental resolution of about 3.5 meV indicated in the figure.

for a simple cubic lattice, where S is the average spin of Mn ions and a is the Mn-Mn bond distance. We get $JS = 4.9$ meV. If we only fit the low- q data up to $q < 0.2$ r.l.u. by the dispersion valid for a simple nearest-neighbor Heisenberg model

$$\hbar\omega(q) = \Delta + 4JS(1 - \cos 2\pi q_h) \quad (4)$$

with $q = (q_h, 0, 0)$, then by fixing $\Delta = 0.20$ meV we get $JS = 5.8$ meV. Now fixing these values of $\Delta = 0.20$ meV and $JS = 5.8$ meV we have calculated the dispersion which is plotted as a continuous curve in Fig. 2. This gives a zone-boundary energy of about 46.7 meV which is higher than the experimental zone-boundary energy of about 35 meV. So there is a clear softening of the spin waves at the zone

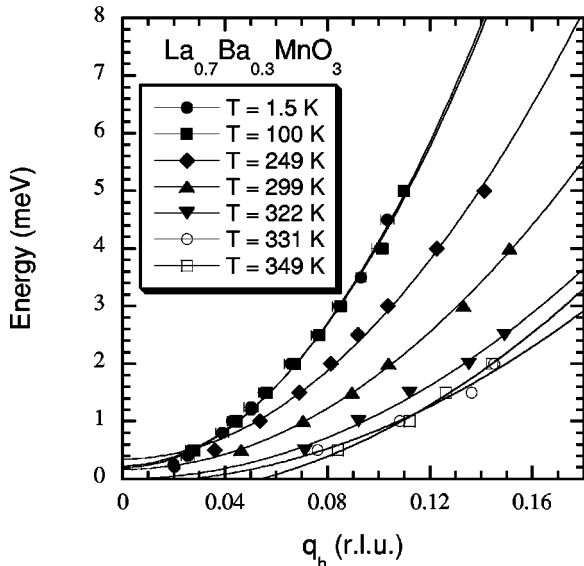


FIG. 5. Low- q dispersion of the acoustic branch of the magnetic excitations in $\text{La}_{0.7}\text{Ba}_{0.3}\text{MnO}_3$ along $[100]$ at several temperatures.

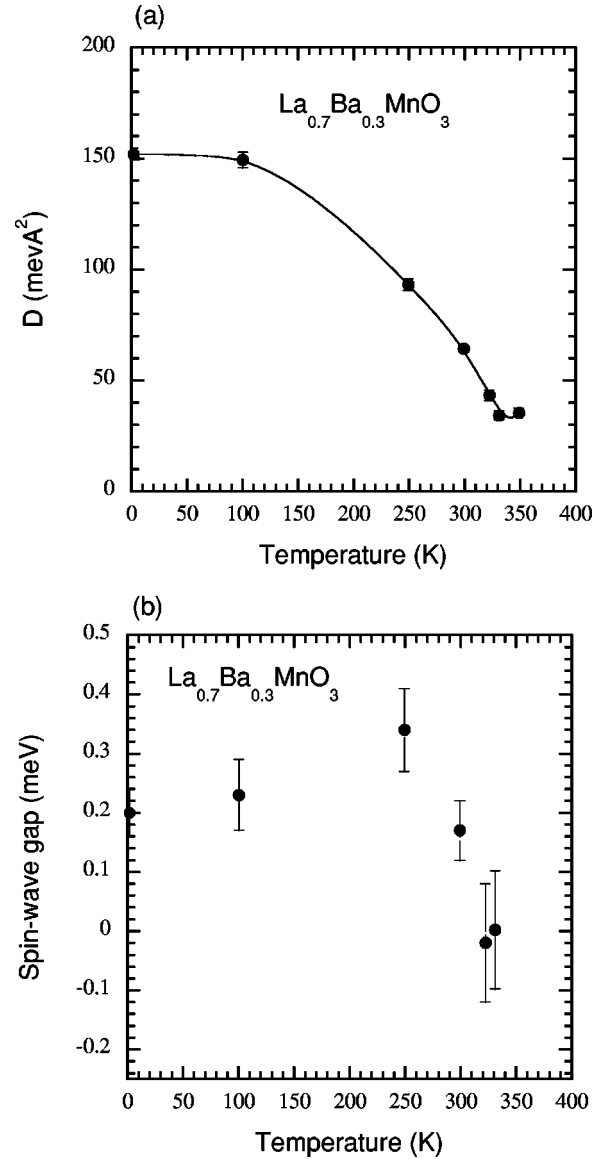


FIG. 6. Temperature variation of (a) the spin-wave stiffness constant D and (b) the energy gap Δ of the acoustic mode of the magnetic excitations in $\text{La}_{0.7}\text{Ba}_{0.3}\text{MnO}_3$ along $[100]$ obtained by fitting Eq. (2) to the low- q dispersion data. The continuous curve in (a) is just a guide to the eyes.

boundary. If we vary Δ and $4JS$ and fit by the least squares the data points by Eq. (4) then we get $\Delta = 1.5 \pm 0.7$ meV and $4JS = 15.1 \pm 0.7$ meV or $JS = 7.8 \pm 0.4$ meV. The fit which is shown by the dotted curve in Fig. 2 is not very good suggesting that the simple Heisenberg model is not valid. Also the fitted gap Δ is much higher than the value $\Delta = 0.20 \pm 0.04$ by using low- q data obtained from cold triple-axis measurements. However, the exchange interaction obtained is about of the same value as that obtained¹³ in $\text{La}_{0.3}\text{Pb}_{0.3}\text{MnO}_3$. We have measured the dispersion of the spin wave along $[110]$ with the thermal triple-axis spectrometer only. The dispersion along $[110]$ which is shown in Fig. 3. The continuous curve has been calculated from the equation

$$\hbar\omega(q) = \Delta + 8JS(1 - \cos 2\pi q_{hh}), \quad (5)$$

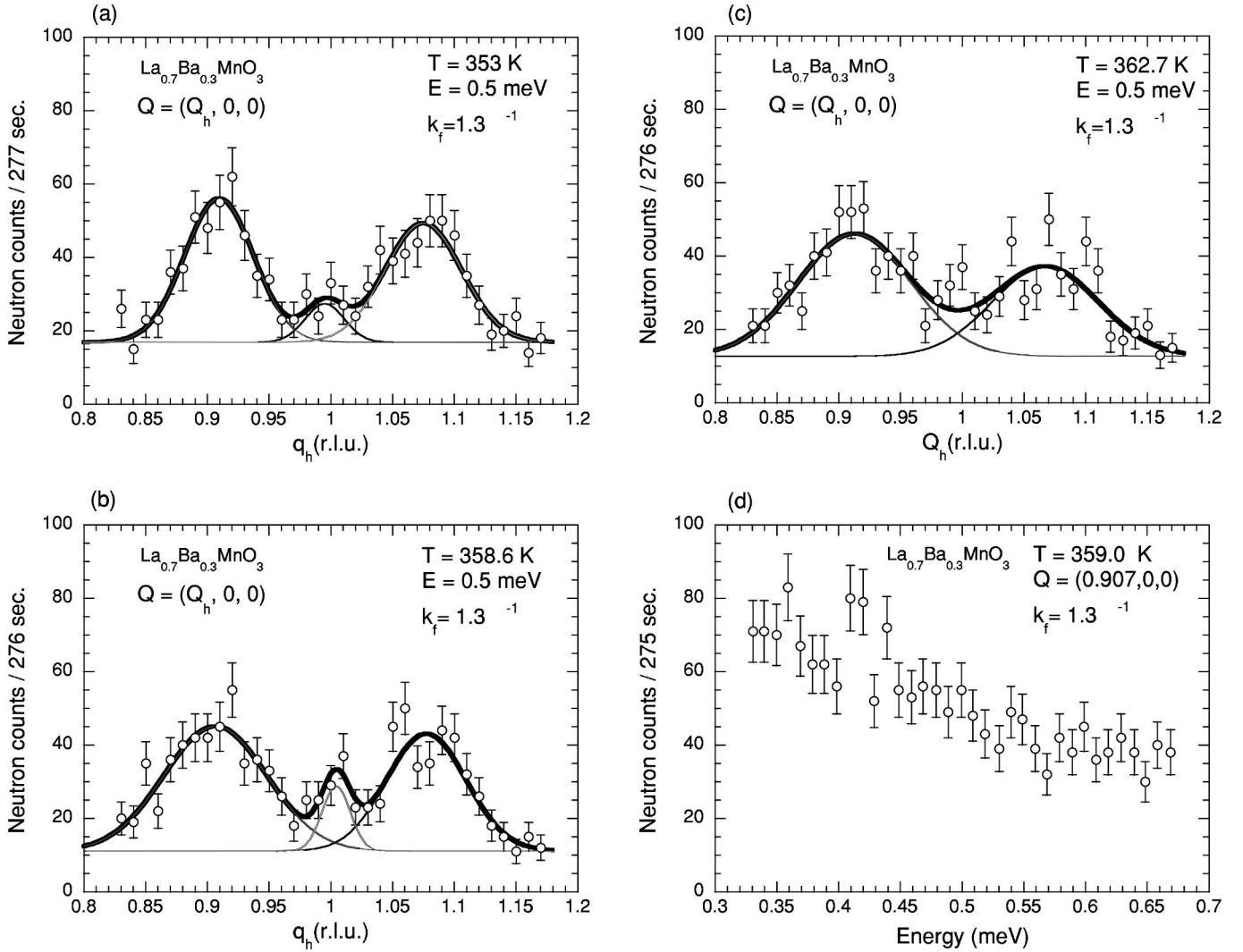


FIG. 7. Constant-energy scans of the magnetic excitations in $\text{La}_{0.7}\text{Ba}_{0.3}\text{MnO}_3$ above $T_C \approx 350$ K at (a) $T = 353$ K, (b) $T = 358$ K, and (c) $T = 362.7$ K with an energy transfer of 0.5 meV. (d) shows a constant- Q scan at $Q = (0.907, 0, 0)$ at $T = 359$ K.

with $q = (q_{hh}, q_{hh}, 0)$ by fixing $\Delta = 0.20$ meV and $JS = 5.8$ meV obtained from the low- q data along $[100]$. Since we do not have high- q data along $[110]$ we could not determine the softening of the spin-waves at the zone boundary in the same way we have determined the softening along $[100]$ outlined above. Figure 4 gives a typical energy scan at $Q = (1.55, 0, 0)$ at $T = 1.5$ K. The full width at the half maximum (FWHM) of the energy scan is 20 ± 2 meV which is much larger than the instrumental resolution of about 3.5 meV shown in Fig. 4. This demonstrates that the spin waves in $\text{La}_{0.7}\text{Ba}_{0.3}\text{MnO}_3$ are heavily damped. These results are in agreement with those obtained in other three-dimensional^{14,15} and bilayer manganites.^{21–23}

We have measured the low- q dispersions of $\text{La}_{0.7}\text{Ba}_{0.3}\text{MnO}_3$ at several temperatures in the temperature range 1.5–250 K on the cold triple-axis spectrometer. We have determined the spin-wave stiffness constant D by fitting the data with Eq. (3). Figure 5 shows the dispersions at several temperatures and the fitted curves. The resulting spin wave stiffness constant D has been plotted as a function of temperature in Fig. 6(a). The spin-wave stiffness remains

constant ($D = 152 \pm 3$ meV \AA^2) at low temperature at least up to $T = 100$ K. At higher temperature D decreases continuously. Figure 6(b) shows the temperature variation of the gap Δ . The energy gap decreases with temperature and becomes zero at $T_C \approx 350$ K. The measurement of D becomes unreliable close to $T_C \approx 350$ K. The ratio $D/kT_C = 5.04$ \AA^2 is rather high as is expected for an itinerant ferromagnet. The ratio $D/kT_C = 3.19$ and 10.1 \AA^2 for itinerant ferromagnet iron and nickel and $D/kT_C = 2.01$ and 1.82 \AA^2 for localized ferromagnet EuO and EuS, respectively.^{22,24}

We performed constant-energy scans above $T_C \approx 350$ K at $T = 353$, 359, and 363 K with an energy transfer of 0.5 meV which are shown in Fig. 7. All these scans showed well-defined peaks at $Q = (1 \pm \delta, 0, 0)$ and small peaks at $Q = (1, 0, 0)$. However, a constant- Q energy scan at $Q = (0.907, 0, 0)$ at $T = 359$ K, which is also shown in Fig. 7, did not reveal any convincing peak structure at $E = 0.5$ meV. Instead we observed continuous decrease in intensity. It is likely that we missed the peak due to the narrow scan width chosen. The absence of the peak structure is also

not surprising because similar results were reported decades earlier in itinerant ferromagnet nickel and iron above T_C .²⁵⁻²⁸ The paramagnetic scattering seems to have ridge-like structure in the E - q plane and needs to be further investigated taking special care about the role of the instrumental resolution.

In conclusion, we have determined the spin wave dispersions of the CMR ferromagnet $\text{La}_{0.7}\text{Ba}_{0.3}\text{MnO}_3$ at 1.5 K along the pseudocubic [100] and [110] directions and also their temperature dependence. We have determined an effective nearest-neighbor exchange constant by using a localized Heisenberg model to fit the data. The quality of the fit shows

that the localized Heisenberg model is unable to fit the experimental dispersion adequately in the whole q range. The magnons show softening at the zone boundary and are heavily damped for higher q . The zone-boundary softening and damping seem to be generic features of the double-exchange ferromagnets including those with high value of T_C . This agrees qualitatively with the minimal double-exchange model^{8,23} with quantum and thermal corrections.

We thank S. A. Guretskii for providing us with the $\text{La}_{0.7}\text{Ba}_{0.3}\text{MnO}_3$ single crystal. T.C. wishes to thank Dr. G. Jackeli and Dr. N. Shannon for critical discussions.

-
- ¹ *Colossal Magnetoresistive Oxides*, edited by Y. Tokura (Gordon and Breach, New York, 2000).
- ² *Colossal Magnetoresistance, Charge Ordering and Related Properties of Manganese Oxides*, edited by C.N.R. Rao and B. Raveau (World Scientific, Singapore, 1998).
- ³ F. Moussa and M. Hennion, in *Colossal Magnetoresistive Magnetites*, edited by T. Chatterji (Kluwer Academic Publishers, Dordrecht, in press), and references therein; M. Hennion, F. Moussa, G. Biotteau, J. Rodriguez-Carvajal, L. Pinsard, and A. Revcolevschi, Phys. Rev. B **61**, 9513 (2000); M. Hennion, F. Moussa, G. Biotteau, J. Rodriguez-Carvajal, L. Pinsard, and A. Revcolevschi, Phys. Rev. Lett. **81**, 1957 (1998); F. Moussa, M. Hennion, G. Biotteau, J. Rodriguez-Carvajal, L. Pinsard, and A. Revcolevschi, Phys. Rev. B **60**, 12 299 (1999); M. Hennion, F. Moussa, J. Rodriguez-Carvajal, L. Pinsard, and A. Revcolevschi, *ibid.* **56**, R497 (1997); F. Moussa, M. Hennion, J. Rodriguez-carvajal, H. Moudou, L. Pinsard, and A. Revcolevschi, *ibid.* **54**, 15 149 (1996); L. Vasiliu-Doloc, J.W. Lynn, A.H. Moudou, A.M. de Leon-Guevara, and A. Revcolevschi, *ibid.* **58**, 14 913 (1998); J.W. Lynn, R.W. Erwin, J.A. Borchers, Q. Huang, A. Santoro, J.-L. Peng, and Z.Y. Li, Phys. Rev. Lett. **76**, 4046 (1996); K. Hirota, N. Kaneko, A. Nishizawa, and Y. Endo, J. Phys. Soc. Jpn. **65**, 3736 (1996); M.C. Martin, G. Shirane, Y. Endoh, K. Hirota, Y. Moritomo, and Y. Tokura, Phys. Rev. B **53**, R14 285 (1996); Y. Endoh and K. Hirota, J. Phys. Soc. Jpn. **66**, 2264 (1997).
- ⁴ C.S. Zener, Phys. Rev. **82**, 403 (1951).
- ⁵ P.W. Anderson and H. Hasegawa, Phys. Rev. **100**, 675 (1955).
- ⁶ P.G. de Gennes, Phys. Rev. **100**, 564 (1955).
- ⁷ N. Furukawa, J. Phys. Soc. Jpn. **65**, 1174 (1996).
- ⁸ N. Shannon and A.V. Chubukov, J. Phys.: Condens. Matter **14**, L235 (2002); N. Shannon and A.V. Chubukov, Phys. Rev. B **65**, 104418 (2002).
- ⁹ D.I. Golosov, Phys. Rev. Lett. **84**, 3974 (2000).
- ¹⁰ T.A. Kaplan and S.D. Mohanti, J. Phys.: Condens. Matter **9**, L291 (1997).
- ¹¹ P. Wirth and E. Müller-Hartmann, Eur. Phys. J. B **5**, 403 (1998); D. Golosov, J. Appl. Phys. **87**, 5804 (2000).
- ¹² Y. Motome and N. Furukawa, J. Phys. Soc. Jpn. **71**, 1419 (2002).
- ¹³ T. Perring, G. Aeppli, S.M. Hayden, S.A. Carter, J.P. Remeika, and S.-W. Cheong, Phys. Rev. Lett. **77**, 711 (1996).
- ¹⁴ H.Y. Hwang, P. Dai, S.-W. Cheong, G. Aeppli, D.A. Tennant, and H.A. Mook, Phys. Rev. Lett. **80**, 1316 (1998).
- ¹⁵ P. Dai, H.Y. Hwang, J. Zhang, J.A. Fernandez-Baca, S.-W. Cheong, C. Kloc, Y. Tomioka, and Y. Tokura, Phys. Rev. B **61**, 9553 (2000).
- ¹⁶ R. von Helmolt, J. Wocker, B. Holzapfel, M. Schultz, and K. Samwer, Phys. Rev. Lett. **71**, 2331 (1993).
- ¹⁷ B. Dabrowski, K. Rogacki, X. Xiong, P.W. Klamut, R. Dybziński, J. Shaffer, and J.D. Jorgensen, Phys. Rev. B **58**, 2716 (1998).
- ¹⁸ H.L. Ju *et al.*, J. Magn. Magn. Mater. **219**, 1 (2000).
- ¹⁹ P.G. Radaelli *et al.*, J. Solid State Chem. **122**, 444 (1996).
- ²⁰ A.A. Arsenov, N.G. Behenin, V.S. Gaviko, V.V. Mashkautsan, Ya.M. Mukovskii, D.A. Shulytev, V.V. Ustinov, R.I. Zainuliina, C.P. Adams, and J.W. Lynn, Phys. Status Solidi A **189**, 673 (2002).
- ²¹ T. Chatterji, L.P. Regnault, P. Thalmeier, R. Suryanarayanan, G. Dhalenne, and A. Revcolevschi, Phys. Rev. B **60**, R6965 (1999).
- ²² T. Chatterji, L.P. Regnault, P. Thalmeier, R. van de Kamp, W. Schmidt, A. Hiess, P. Vorderwisch, R. Suryanarayanan, G. Dhalenne, and A. Revcolevschi, J. Alloys Compd. **326**, 15 (2001).
- ²³ N. Shannon, T. Chatterji, F. Ouchni and P. Thalmeier, Eur. Phys. J. B **27**, 287 (2002).
- ²⁴ H.A. Mook, in *Spin Waves and Magnetic Excitations I*, edited by A.S. Borovik-Romanov and S.K. Sinha (Elsevier, Amsterdam, 1988), p. 425.
- ²⁵ H.A. Mook, J.F. Lynn, and R.M. Nicklow, Phys. Rev. Lett. **30**, 556 (1973).
- ²⁶ J.W. Lynn and H.A. Mook, Phys. Rev. B **23**, 198 (1981).
- ²⁷ J.W. Lynn, Phys. Rev. B **11**, 2624 (1975).
- ²⁸ G. Shirane, O. Steinsvoll, Y.J. Uemura, and J. Wicksted, J. Appl. Phys. **55**, 1887 (1984).